arXiv:1509.00356v2 [nucl-th] 10 Nov 2015

The Quarkyonic Star

Kenji Fukushima
Department of Physics, The University of Tokyo, 7-3-1 Hongo, Bunkyo-ku, Tokyo 113-0033, Japan
fuku@nt.phys.s.u-tokyo.ac.jp

Toru Kojo
Department of Physics, University of Illinois at Urbana-Champaign, 1110 W. Green Street, Urbana, Illinois 61801, USA
torukojo@illinois.edu

ABSTRACT

We discuss theoretical scenarios on crossover between nuclear matter (NM) and quark matter (QM). We classify various possibilities into three major scenarios according to the onset of diquark degrees of freedom that characterizes color-superconducting (CSC) states. In the conventional scenario NM occurs at the liquid-gas (or liquid-vacuum at zero temperature) phase transition and QM occurs next, after which CSC eventually appears. With the effect of strong correlation, the BEC-BCS scenario implies that CSC occurs next to NM and QM comes last in the BCS regime. We adopt the quarkyonic scenario in which NM, QM, and CSC are theoretically indistinguishable and thus these names refer to not distinct states but relevant descriptions of the same physical system. Based on this idea we propose a natural scheme to interpolate NM near normal nuclear density and CSC with vector coupling at high baryon density. We finally discuss the mass-radius relation of the neutron star and constraints on parameters in the proposed scheme.

Subject headings: Neutron star, Equation of state, Nuclear matter, Quark matter, Color superconductor

1. Introduction

Quantum chromodynamics (QCD) is one fundamental theory in the Standard Model in which non-Abelian gauge fields (gluons) and fermions (quarks) interact non-perturbatively and QCD-related phenomena are characterized by an energy scale; $\Lambda_{\rm QCD} \simeq 0.2$ GeV. The QCD-vacuum has a rich structure with a variety of condensates and it dynamically confines any colored excitation. At finite temperature of $T \sim \Lambda_{\rm QCD}$ and low baryon density of $n_{\rm B} \ll \Lambda_{\rm QCD}^3$, ultra-relativistic nucleus-nucleus collision at Relativistic Heavy-Ion Collider called RHIC and Large Hadron Collider called LHC, supported by the lattice-QCD Monte-Carlo calculations, has revealed quantitative properties of a novel strongly-correlated state of QCD matter, hadronic gas at $T \lesssim \Lambda_{\rm QCD}$ and the quark-gluon plasma (QGP) at $T \gtrsim \Lambda_{\rm QCD}$. In contrast, when $T \ll \Lambda_{\rm QCD}$ and $n_B \sim \Lambda_{\rm QCD}^3$, our knowledge from QCD is severely limited because the first-principle numerical method based on the importance sampling fails at finite baryon density. Therefore, it is important to impose constraints on theoretical uncertainties from the experimental side such as the neutron star observation and the beam-energy scan program at RHIC and future heavy-ion facilities. The purpose of this paper is to import the state-of-the-art idea of color deconfinement phenomenon at high T and high $n_{\rm B}$, especially a special feature of dense and large-$N_{\rm c}$ QCD, into the neutron star phenomenology, which in turn provides us with useful constraints.

In some limiting cases at low and high baryon densities we have reasonable understanding of cold QCD matter. At $n_{\rm B} = (1 \sim 2)n_0$ (where $n_0 \simeq 0.16$ fm^{-3} is the nuclear saturation density), on

the one hand, one can utilize empirical knowledge from nuclear physics and well-developed theoretical methods to analyze nuclear matter (NM) properties (Weinberg 1990; Epelbaum et al. 2009). Recent developments include not only the chiral perturbation theory (Fiorilla et al. 2012; Krueger et al. 2013) and the chiral effective model (Lastowiecki et al. 2015; Holt et al. 2014) but also the functional renormalization group (Drews & Weise 2015). On the other hand, at asymptotically high density $n_B \gtrsim 100 n_0$ (or even smaller densities hopefully), perturbative QCD (pQCD) calculations are validated for the bulk quantities of quark matter (QM) as seen from the convergence of three-loop perturbative results (Freedman & McLerran 1977; Kurkela et al. 2010; Fraga et al. 2015). Besides, pQCD works well to describe the color-superconducting (CSC) states. In particular the ground state of QCD in the high-density limit has been identified as the color-flavor-locked (CFL) state (Alford et al. 1999b) (see also a review by Fukushima & Hatsuda (2011) and references therein).

The most problematic is the QCD matter study in the intermediate density region: $2n_0 < n_{\rm B} < 100n_0$ or 1.1 GeV $< \mu_{\rm B} <$ 3 GeV in terms of the baryon chemical potential. Neutron stars are unique cosmic laboratories to access such domains experimentally (Buballa et al. 2014). Useful observations include the mass-radius (M-R) relation, the cooling curve (Shternin et al. 2011; Page et al. 2004, 2006, 2011; Tsuruta et al. 2002; Blaschke et al. 2000, 2004), the surface and toroidal magnetic fields (Duncan & Thompson 1992; Cardall et al. 2001; Olausen & Kaspi 2014; Kitamoto et al. 2014), the gravitational waves from the merger of binary neutron stars (Abbott et al. 2009; Hotokezaka et al. 2011, 2013), and so on. In the present work we will specifically pay our attention to the mass-radius relation.

The interesting point of the M-R relation is that it has a one-to-one correspondence to the the QCD equation of state (EoS) through the Tolman-Oppenheimer-Volkoff (TOV) equation. The overall size of neutron star radii is determined by the EoS around $n_B = (1 \sim 2)n_0$ (Lattimer & Prakash 2001, 2007), while the typical neutron star masses $M \gtrsim M_\odot$ (where $M_\odot$ denotes the solar mass) are largely correlated with the pressure at the central cores with $n_B = (2 \sim 10)n_0$. According to the discoveries of PSR J1614-2230 (Demorest et al. 2010) and PSR J0348+0432 (Antoniadis et al. 2013) there should be neutron stars whose mass exceeds $2M_\odot$, indicating that the QCD EoS must be very stiff at $n_B > 2n_0$ as compared to what was naïvely considered.

The requirement of stiffness challenges conventional EoS's beyond the nuclear regime. In typical hadronic models the strangeness appears at $n_{\rm B} = (2 \sim 3)n_0$ (Glendenning & Schaffner-Bielich 1999, 1998; Tsubakihara et al. 2010), which significantly softens the EoS (i.e., hyperon puzzle). Seminal works (Nishizaki et al. 2002; Vidana et al. 2011; Weissenborn et al. 2012; Yamamoto et al. 2014; Lonardoni et al. 2015) introduced repulsive interactions of strangeness to circumvent the hyperon puzzle, and the results imply that the repulsion not only in two-body force of baryons but also in three- and more-body forces are necessary to pass the $2M_\odot$ constraint. While many-body forces including hyperons have been poorly constrained, new data on the nucleon-hyperon scattering and hypernuclei at J-PARC (Nagae 2010; Tamura 2010; Nakazawa & Takahashi 2010) as well as the lattice simulations at the physical quark masses (Inoue et al. 2012; Beane et al. 2013) will provide important clues to resolve the hyperon puzzle.

In general contributions from many-body force of baryons starts growing rapidly at $n_{\rm B} \sim 2n_0$ (Hebeler et al. 2010). From the microscopic point of view strong many-body correlations imply that baryons should exchange many mesons and quarks at $n_{\rm B} \gtrsim 2n_0$. With more and more exchanged quarks, the identity of isolated baryon should be diminished, and quark degrees of freedom gradually take over physical degrees of freedom. Eventually, baryons with the radii $(0.5 \sim 0.8)$ fm begin to overlap with each other at $n_{\rm B} \gtrsim (5 \sim 10)n_0$, leading to the percolated quark matter (Baym & Chin 1976). This physics picture contrasts with other crossover scenarios and fills smoothly in a gap between nuclear and quark matter with exchanged mesons and quarks. The matter in the confinement/deconfinement crossover domain should inherit properties from both nuclear and quark matter. The idea of *quarkyonic matter*, that was first recognized by McLerran & Pisarski (2007), is an important step toward correct understanding of the crossover, as we will closely discuss later. We

will further push this idea forward concrete implementation to construct an EoS.

In this paper we delineate the crossover scenario bridged by quarkyonic matter. As we emphasize later, the most essential point in this scenario is that there exists an overlapping region that can be described in terms of strongly-interacting baryons or strongly-interacting quarks equally. For a concrete realization we utilize an Nambu–Jona-Lasinio (NJL) type model including vector and diquark interactions (for a review, Buballa (2005)) which are generally density dependent. Applying the quark-hadron duality picture we determine the low-density behavior of parameters by fitting the Akmal-Pandaripande-Ravenhall (APR) nuclear EoS (Akmal et al. 1998). The high-density behavior is constrained by confronting the EoS with the $2M_\odot$ constraint. In this way we cast the M-R relation onto the quark model parameters, and we analyze the transitional behavior with increasing density.

One robust conclusion from our analysis is that the interactions should remain large even at $n_{\rm B} \sim 10n_0$ to account for the existence of massive neutron stars. One might consider that the asymptotic freedom in QCD would rather validate weakly interacting picture just in percolated quark matter, since the typical distance among quarks is small. Such intuition, however, does not always work unless soft gluon contributions are cutoff. For instance, in high-T QCD matter magnetic gluons remain unscreened and non-perturbative contributions survive even for asymptotically high temperature (Hietanen et al. 2009). Also QCD in two-dimensions as an asymptotic free theory ('t Hooft 1974) has dense quark matter in which non-perturbative gluons survive to asymptotically high density, since in spatially one-dimension screening effects are not enhanced at finite density (Schon & Thies 2000; Bringoltz 2009; Kojo 2012). In dense QCD, while the hard-dense-loop (HDL) type calculations at weak coupling predict the electric screening mass of the QCD coupling constant times quark chemical potential, $\sim g_s\mu_q$, actually the soft region in the gluon polarization function is highly dependent on the non-perturbative physics near the quark Fermi surface and can deviate from the HDL results at *qualitative* level (Rischke et al. 2001; Huang & Shovkovy 2004b; Fukushima 2005; Kojo & Baym 2014). Therefore the significance of the screening effects is still an open question until first-principle calculation determines the phase structure. In this situation it should be useful to construct an argument in which non-perturbative gluons survive in percolated quark matter, as discussed in the quarkyonic scenario. In this paper we try to address this issue from the neutron star phenomenology, and use the $2M_\odot$ constraint to discuss why non-perturbative gluons should survive to $n_B \sim 10n_0$.

The treatment of the crossover EoS proposed in the present work has some overlap with preceding works. The attempts to directly interpolate pQCD and nuclear EoS have been made by Freedman & McLerran (1978); Fraga et al. (2015). Also Alford et al. (2005) discussed that an EoS for quark matter with CSC can mimic the APR EoS. In these studies the descriptions of quark matter are based on the extrapolation of the pQCD picture. On the other hand, recent studies on the crossover scenario have used more model dependent but direct descriptions to conceptualize strongly correlated quark matter for $n_B \gtrsim (3 \sim 5)n_0$, then interpolated the resulting quark EoS and nuclear EoS at $n_B \lesssim 2n_0$ (Masuda et al. 2013b,a, 2015; Alvarez-Castillo et al. 2014; Hell & Weise 2014; Kojo et al. 2015; Kojo 2015). These studies, however, do not manifestly treat microscopic dynamics in the interpolated domain, so one cannot address, for instance, how the strangeness changes in the crossover domain. In the present work we will take a more direct and concrete path to the microscopic description with the interplay among quarks, diquarks, and baryons. We particularly put our emphasis on the role played by diquarks, with which there emerges a natural classification scheme of crossover scenarios as we see below.

This paper is organized as follows. In Sec. 2 we classify the crossover scenarios and discuss the underlying physics. In Sec. 3 we define our model and elucidate how to treat the model parameters. In Sec. 4 we construct an EoS and extract the density dependence of the model parameters. In Sec. 5 we discuss the resulting M-R relations and finally we make concluding remarks in Sec. 6.

2. Quark degrees of freedom beyond nuclear matter

There is no rigorous order parameter for quark deconfinement as soon as dynamical quarks are included in the theory, irrespective of various theoretical efforts (Fukushima 2003). The Polyakov loop serves for an only approximate order parameter at high T, while we have no clue about even an approximate order parameter if the baryon density is high (see also an attempt by Dexheimer & Schramm (2010) to introduce a parameter analogous to the Polyakov loop). Here, we discuss the general features of deconfinement crossover not relying on any models.

2.1. Three scenarios

There is no established understanding on how quarks can become dominating beyond the normal nuclear density where nucleons are the most relevant degrees of freedom. Here we sort out various theoretical speculations on QM into three clearly distinct categories. We particularly pay special attention to the onset of diquark degrees of freedom introducing a diquark binding energy B_d together with a baryon binding energy B_b. Then, we can express the baryon mass as $M_{\rm B} = 3M_{\rm q} - B_b$ and the diquark mass as $M_{\rm d} = 2M_{\rm q} - B_d$, where $M_{\rm q}$ represents the constituent quark mass (Fukushima et al. 2015).

- Conventional scenario (NM < QM < CSC): In CSC at weak coupling QM is assumed to overcome NM beyond some baryon density. Once we admit it, we can see that the Cooper instability suggests strong correlation of diquarks in momentum space. This, however, does not necessarily imply that those diquarks are localized in space or bound states. In fact we usually have $B_d < 0$ in the BCS-type calculation, leading to the following ordering: $M_{\rm B}/3 < M_{\rm q} < M_{\rm d}/2$. Therefore, there should be an onset for QM next to the liquid-gas transition of NM. Such an onset is implemented in quark models or a first-order phase transition between NM and QM around $\mu_{\rm B} \sim 3M_{\rm q}$ (with minor in-medium corrections) is often assumed to construct an EoS. At higher baryon density, eventually, diquarks form a condensate in the CSC states.

- BEC-BCS scenario (NM < CSC < QM): In the intermediate region of baryon density the weak-coupling study may be drastically altered. If the attractive interaction is strong enough, the Cooper pair could become localized in space and then CSC is identified as a Bose-Einstein condensate (BEC) of bound diquarks (Abuki et al. 2002), which is called a (quasi-)molecule in condensed matter physics systems controlled by a Feshbach resonance (Ohashi & Griffin 2002). Then, we should anticipate a crossover transition between the BCS and the BEC regimes as the coupling strength changes (Nishida & Abuki 2005; Kitazawa et al. 2008; Sun et al. 2007). In the BEC regime where $B_d > 0$, the mass hierarchy should be reorganized as: $M_{\rm B}/3 < M_{\rm d}/2 < M_{\rm q}$. This is actually a situation in some descriptions using quark-meson-diquark models in which diquarks are considered as physical degrees of freedom (Fukushima et al. 2015).

- Quarkyonic scenario (NM ∼ QM ∼ CSC): It is also a speculative but logical possibility that interacting nucleons are, in principle, indistinguishable from matter out of quarks. One heuristic measure to characterize quark deconfinement is the mobility of hadrons and quarks (Karsch & Satz 1980). Then, quarks can always hop from one nucleon to the other via meson exchange. In this sense the mobility of quarks is never vanishing as long as nucleons are interacting. One can upgrade this hand-waving argument to a more precise formulation by taking the large-$N_{\rm c}$ limit, which makes clear the difference between the high-T low-$\mu_{\rm B}$ situation and the low-T high-$\mu_{\rm B}$ situation. In the former case mesons become non-interacting objects in the large-$N_{\rm c}$ limit, so that quark deconfinement is well-defined by percolation of overlapping wave-functions of mesons. In the latter case at high baryon density, on the other hand, the interaction among nucleons is of $\mathcal{O}(N_{\rm c})$ leading to a large pressure of $\mathcal{O}(N_{\rm c})$ that is comparable to the pressure of quark matter (McLerran & Pisarski 2007). This is a natural consequence from the fact that nucleon interactions are induced by quark exchange, and thus the pressure of nuclear

matter should be sensitive to quark degrees of freedom. This important observation on the pressure of $\mathcal{O}(N_c)$ of both nuclear and quark matter opens a third scenario that there should be a regime of *duality* in which nuclear matter can be equivalently described in terms of quarks and diquarks (i.e., the McLerran-Pisarski conjecture as advocated by Fukushima & Sasaki (2013)). Such a special regime in the intermediate baryon density is called the quarkyonic regime.

In this work we adopt this last picture of the quarkyonic scenario. There are three reasons why we consider that the quarkyonic scenario should be the most realistic:

(1) Center symmetry is more and more badly broken with increasing baryon density, and so the deconfinement phenomenon at high baryon density should be even broader crossover than that at high temperature. Thus, a first-order phase transition to quark matter is quite unlikely. In many models the chiral phase transition at low temperature could be of first order, but once a reasonable amount of vector coupling is included, it also becomes smooth crossover (Kitazawa et al. 2002; Sasaki et al. 2007; Fukushima 2008; Bratovic et al. 2013). Also, the CSC phase can be smoothly connected to the confined phase; for example SU(N) lattice gauge theories coupled to fixed-length Higgs fields have a crossover region between confined and Higgs phase (Fradkin & Shenker 1979). Therefore, it is the most conceivable that nucleons are gradually taken over by more fundamental degrees of freedom.

(2) It is highly non-trivial how to reconcile confinement and the BEC-BCS crossover. To form bound states of diquarks, the inter-quark interaction should be strong, and then, the interaction among any colored objects including diquarks must be strong as well. Then, all the colored objects are expected to form color-singlet bound states. Theoretically speaking, however, what we can observe in principle is only the gauge invariant quantity and so there is no way to judge whether quarks and diquarks are confined in color-singlet bound states or not. This at the same time means that we cannot exclude a mixture of quarks and diquarks even in the confined phase where the interaction is strong.

(3) The hadron resonance gas model is known to be successful to reproduce the thermodynamic properties of hadronic matter near or even slightly above T_c for small μ_B (for a recent review, see Ding et al. (2015)). This is a clear example of the duality between hadrons and quarks in a transitional regime. From this point of view we can say that the quarkyonic regime could be a high-density counterpart of the so-called strongly-correlated QGP (i.e., sQGP) established in RHIC experiments. This analogy between sQGP and quarkyonic matter is addressed by Fukushima (2014).

2.2. Quark-hadron continuity

From the point of view of the symmetry-breaking pattern we can give some more solid arguments to justify the quarkyonic scenario which is quite consistent with the CSC theory. It has been a closely investigated conjecture called the quark-hadron continuity that the superfluid nuclear matter is a dual state of the CFL phase (Schaefer & Wilczek 1999; Alford et al. 1999a; Fukushima 2004; Hatsuda et al. 2006). The point is that the superfluid nuclear matter and the CFL phase break chiral symmetry and $U(1)_B$ symmetry. The theoretical description based on the symmetries is elegant and convincing only in the chiral limit, but the strange quark mass comparable to Λ_{QCD} introduces subtlety. In particular the CFL phase may not continue to the normal nuclear density due to the Fermi surface mismatch. Then, possibilities include a CFL state entering the gapless region which is known to suffer instabilities against spatial modulation (Fukushima et al. 2005; Huang & Shovkovy 2004a; Fukushima 2005). If the interaction is sufficiently strong, the instability might be avoided (Gubankova et al. 2006).

In this work we postulate a large enough value of the diquark coupling H, so that we do not have to cope with instability problems. Then, there should be a phase transition to the two-flavor super-conducting (2SC) phase down from the CFL phase as lowering the baryon density. The pure 2SC phase has diquark condensates of ru-gd and rd-gu quark pairs in color space of red and green and in flavor space of up and down. Within the two-flavor sector these combinations in flavor space are SU(2) singlets, and so none of $SU(2)_L \times SU(2)_R$ is broken. Besides, $U(1)_B$ is broken but a modified $U(1)_{\tilde{B}}$ is kept unbro-

ken, where $\mathrm{U}(1)_{\tilde{\mathrm{B}}}$ is generated by a mixed charge $\tilde{B} = B - 2Q_e$. In fact, the diquarks ru-gd and rd-gu have $B = 1/3 + 1/3 = 2/3$, the electric charge $Q_e = 2/3 - 1/3 = 1/3$ in unit of e, and therefore $\tilde{B} = 0$. Hence, no global symmetry is broken in the 2SC phase.

It is also possible to have not the pure 2SC phase but the coexisting 2SC phase with non-zero chiral condensates. In this case chiral symmetry is spontaneously broken by the chiral condensates, and the diquark condensate breaks no new symmetry. Thus, the coexisting 2SC phase has a completely identical pattern of the symmetry breaking as the hadronic phase. In other words we have no way to exclude the 2SC-type diquark condensate even in NM in the confined phase. Considering the strange quark mass, such continuity between the coexisting 2SC phase and NM should be a more realistic candidate than the CFL-NM continuity. In conclusion, the quarkyonic scenario based on deconfinement is supported from the chiral symmetry point of view by the presence of the coexisting 2SC phase with non-zero chiral condensates.

Here, let us make two remarks to clarify possibly confusing points. The first point is the order parameter and gauge symmetry. In the mean-field approximation there can be a phase transition between normal QM and the 2SC phase and the associated order parameter is the diquark condensate. So, one might think that there should be also a phase transition from NM to the 2SC phase even though the symmetry has no difference. This is true only approximately as long as one fixes the gauge and relies on the mean-field approximation. However, generally beyond the mean-field level, there is no gauge-invariant order parameter for the 2SC phase while one could construct higher dimensional order parameters for the CFL phase (Rajagopal & Wilczek 2000; Fukushima & Hatsuda 2011; Fukushima 2004). This "non-existence" of the 2SC order parameter strongly suggests crossover between NM and the 2SC phase, which is reminiscent of the non-existence of the exact order parameter and smooth crossover of deconfinement at high temperature.

The next remark is about the consistency of the quarkyonic regime that was recognized in the large-N_c limit and the CSC that is disfavored in the large-N_c limit. This is sometimes a source of conceptual confusion. To discuss the quarkyonic regime we do not have to take the large-N_c limit; while the quarkyonic picture was initially studied in the large-N_c limit, its implication is more general and the essence can be discussed even in two-color QCD (Brauner et al. 2009; Hands et al. 2010). If NM and the 2SC phase are identifiable, we should consider that this continuity between NM and the 2SC phase is nothing but a clear realization of the quarkyonic regime in the real world with three colors. This point is emphasized by Fukushima (2014) and is precisely the physics picture that we make full use of in the present work.

3. Model and parameters

In the low density region we adopt the EoS of nuclear matter, and in this section let us explain how we compute the EoS of QM at high baryon density. We will treat the NJL model within the mean-field approximation (for details, see e.g. Buballa (2005); Klahn et al. (2007); Kojo (2015)). We have three gap energies, Δ_{ud}, Δ_{ds}, and Δ_{su}, associated with diquark condensates. Moreover, we should introduce three chiral condensates, $\langle\bar{u}u\rangle$, $\langle\bar{d}d\rangle$, and $\langle\bar{s}s\rangle$, which are all dynamically determined from the gap equations. As we discuss in details, the vector coupling is an essential ingredient for our prescription, so we need to treat $n = \langle\bar{q}\gamma^0 q\rangle$ as a mean-field variable, as well as three chemical potentials μ_e, μ_3, and μ_8 to impose electric and color charge neutrality. Therefore, in total, there are ten mean-field variables and we must solve ten gap equations simultaneously.

With these mean-field variables (with a notation; $\phi_u = \langle\bar{u}u\rangle$, $\phi_d = \langle\bar{d}d\rangle$, and $\phi_s = \langle\bar{s}s\rangle$) we can write the pressure in the following way:

$$\begin{aligned} P =& \frac{1}{8\pi^2}\int_0^\Lambda dp\, p^2 \sum_{i=1}^{72}\epsilon_i(p) \\ & - G_\mathrm{s}(\phi_u^2+\phi_d^2+\phi_s^2) - 4G_\mathrm{d}\phi_u\phi_d\phi_s + G_\mathrm{v}n^2 \\ & - \frac{1}{H}(\Delta_{ud}^2+\Delta_{ds}^2+\Delta_{su}^2) + P_e + P_\mu\,, \end{aligned} \tag{1}$$

where $\epsilon_i(p)$ represents the energy dispersion relations obtained from the Dirac Hamiltonian in the Nambu-Gorkov doubled basis. The last terms, P_e and P_μ, represent the pressure contributions from electrons and muons.

In the presence of the mean-field n, the quark chemical potential is renormalized as $\mu_r = \mu - 2G_{\rm v}n$. Then, the quark chemical potential takes a from of 9×9 matrix given by

$$\boldsymbol{\mu} = \mu_r \mathbf{1}_{\rm c}\otimes\mathbf{1}_{\rm f} - \mu_e \mathbf{1}_{\rm c}\otimes Q_e + (\mu_3 T_{\rm c}^3 + \mu_8 T_{\rm c}^8)\otimes \mathbf{1}_{\rm f}\,, \tag{2}$$

where $Q_e = {\rm diag}(2/3,-1/3,-1/3)$ is the charge matrix in flavor space. The explicit form of the gap matrix with Δ_{ud}, Δ_{ds}, and Δ_{su} can be found in the literature (Fukushima et al. 2005).

For the model parameters, we use the set of Hatsuda & Kunihiro (1994):

$$\begin{aligned}&\Lambda = 631.4\,{\rm MeV}\,,\quad G_{\rm s}\Lambda^2 = 3.67\,,\quad G_{\rm d}\Lambda^5 = -9.29\,,\\ &m_{u,d} = 5.5\,{\rm MeV}\,,\quad m_s = 135.7\,{\rm MeV}\,,\end{aligned} \tag{3}$$

which are fixed to reproduce hadron phenomenology in the vacuum. The other parameters H and $G_{\rm v}$ are left unfixed, and we will use this freedom to adjust H and $G_{\rm v}$ to realize the quark-hadron duality interpolating the APR and CFL EoS's.

4. Interpolating the EoS with $G_{\rm v}$-running 2SC

Because the CFL solution does not exist in the density region near NM, which indicates a first-order phase transition as discussed later, a natural candidate for the QM ground state there is the 2SC state. As elucidated comprehensively in Sec. 2, the diquark condensate $\langle ud\rangle$ in the 2SC phase breaks no new symmetry and so it can coexist in the hadronic phase. This means that the 2SC phase could be smoothly connected to NM and, furthermore, the quarkyonic scenario requires the presence of duality region where NM and 2SC can represent the same physical system.

It is still non-trivial how to formulate such duality in a practical way. We use the APR hadronic EoS for the baseline, while the 2SC phase has several unconstrained model parameters such as H and $G_{\rm v}$. Our strategy is to make use of these uncertainties positively to reproduce APR in the low density region in a spirit of the quarkyonic scenario. To this end we treat $G_{\rm v}$ in the 2SC phase as a $\mu_{\rm B}$-dependent control parameter and fit the resulting EoS with APR. Besides, we emphasize that this choice of $G_{\rm v}$ as a control parameter would provide us with convenient and transparent intuition about modified QM EoS, and at the same time, that $G_{\rm v}$ should be a *representative* of all unknown effects like confinement near the normal nuclear density. The important point is that in this way, once $G_{\rm v}(\mu_{\rm B})$ is determined, we can smoothly extend APR toward QM without any artificial manipulations.

The pressure P in the 2SC phase depends monotonically on $G_{\rm v}$, so that we can easily find $G_{\rm v}$ that reproduces APR at each $\mu_{\rm B}$. One might think that a $\mu_{\rm B}$-dependent $G_{\rm v}$ may change one of the gap equations, $\partial P/\partial n = 0$. For technical simplicity we do not change the gap equation but treat n as an internal mean-field variable which takes a different value from $n_{\rm B}$. Thus, to obtain $n_{\rm B}$ correctly, we have to compute $\partial P/\partial\mu_{\rm B}$ including the derivative on $G_{\rm v}(\mu_{\rm B})$.

In order to find a suitable running coupling, we found it necessary to take a diquark coupling larger than 1. Otherwise the NJL pressure at any positive $G_{\rm v}$ undershoots APR at typical μ_B, because the NJL effective quark mass, $M_q \simeq 336$ MeV, allows the pressure to develop only when $\mu_B > 3M_q \simeq 1010$ MeV$(> m_N)$ (m_N: nucleon mass). This situation is cured by including the sufficiently large diquark coupling which effectively reduces the effective quark mass (Kojo et al. 2015). Similar effects can be seen in constituent quark models where the color hyper-fine interaction makes the nucleon mass smaller than three times constituent quark mass. We will be interested in $G_{\rm v} \gtrsim 0.5G_{\rm s}$ to achieve sufficient stiffness, and then $H \gtrsim 1.4G_{\rm s}$ is required to pass the $2M_\odot$ and causality constraints. Therefore we will examine $H = 1.5G_{\rm s}$ and $H = 1.6G_{\rm s}$ in the following.

In our fitting procedures one of questions is how to choose the fitting range. Let us first consider a relatively wide fitting range, $\mu_{\rm B} = (1.02\sim 1.20)$ GeV or $n_B \simeq (1.5\sim 3.5)n_0$. (We omitted a very dilute region $\mu_{\rm B} \lesssim 1.02$ GeV because it requires too much fine-tuning in our fit functions.) We show our numerical results with running $G_{\rm v}$ for $H = 1.5G_{\rm s}$ (lower solid curve) and $H = 1.6G_{\rm s}$ (upper solid curve) in Fig. 1. We emphasize that we did not assume any functional form *a priori* and $G_{\rm v}(\mu_{\rm B})$ shown in Fig. 1 results solely from the fit to APR once we make a choice of the diquark coupling H. We vary H to check the sensitivity and will see that this choice is near the upper limit not to violate the causality. It is important

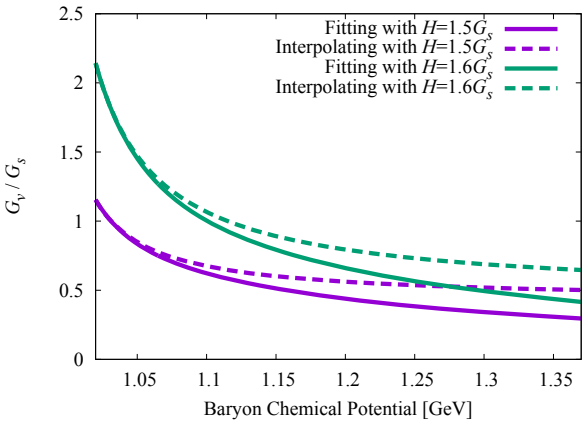

Fig. 1.— Vector coupling in the 2SC phase fitted with APR for $H = 1.5G_{\rm s}$ (lower solid curve) and $H = 1.6G_{\rm s}$ (upper solid curve). The interpolating fit results to the CFL phase with $d = 0.4$ (See Eq.4) are represented by the dotted curves.

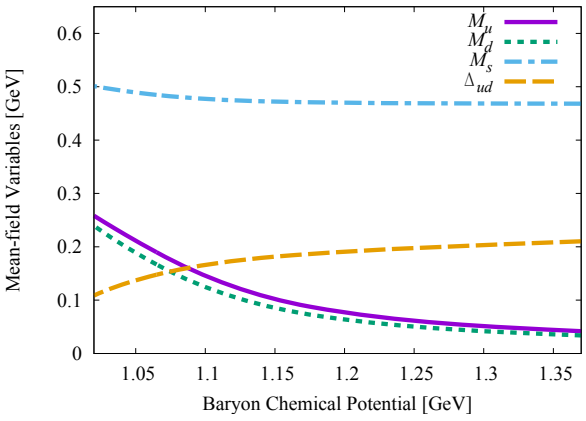

Fig. 2.— Constituent quark masses and the diquark gap Δ_{ud} in the 2SC phase as functions of $\mu_{\rm B}$ in the case of $H = 1.5G_{\rm v}$ (corresponding to the solution shown by a lower solid curve in Fig. 1). The chiral phase transition is a smooth crossover because of the vector coupling.

to note that the chiral phase transition is a very smooth crossover in the presence of large $G_{\rm v}$, so that this 2SC phase can accommodate both diquark and chiral condensates for any $\mu_{\rm B}$. This is clear in Fig. 2 where the constituent quark masses, M_u, M_d, M_s, and the gap energy Δ_{ud} are given as functions of $\mu_{\rm B}$. There is a small discrepancy between M_u and M_d because of the electric charge neutrality condition that breaks isospin symmetry.

Our fit to APR tells us that $G_{\rm v}$ must be very large at low μ_B and relax to $G_{\rm v} \sim 0.5G_{\rm s}$ at large μ_B. The importance of $G_{\rm v}$ can be inferred from nuclear physics (e.g. ω-meson exchange) and typical magnitude $G_{\rm v} \sim 0.5G_{\rm s}$ in our fit is understandable within the conventional context. On the other hand, very large value at low μ_B represents something else and requires explanations. Let us recall that using the diquark coupling we were able to make the onset chemical potential of the NJL pressure close to APR, as required from the quark-hadron duality. But there remains another problem in our fitting procedures; pressure and number density grow much faster in the NJL model than in APR. The obvious reason is the lack of confinement in our model; a quark excites individually, not as a part of a baryon, producing artificial excess of pressure. But large $G_{\rm v}$ can be used to imitate confining effects by tempering the growth of quark number density. This effect should be stronger at lower density; as baryons overlap, $G_{\rm v}$ becomes less responsible for confining effects and should relax to the value expected from the repulsive nuclear forces.

Interestingly, we have found that the best fit form of $G_{\rm v}(\mu_{\rm B})$ is an inverse logarithm for both $H = 1.5G_{\rm s}$ and $H = 1.6G_{\rm s}$. Such an inverse logarithmic is quite suggestive because it is consistent with the common form of the running coupling constant at one-loop level. However, the validity of this fitting should be lost at some point of the baryon density. In fact, at sufficiently high baryon density there is a phase transition from the 2SC to CFL phase which softens the EoS. If we use the running $G_{\rm v}(\mu_{\rm B})$ determined above, the EoS including the CFL phase does not support the massive neutron star with $M \gtrsim 2M_\odot$; $G_{\rm v}$ should be $\sim 0.5G_{\rm s}$ or greater in the CFL phase. Thus we need stiffer 2SC pressure with which the EoS can remain stiff enough even after the transition to the CFL phase occurs.

The above determination used fitting over the range $n_B \simeq (1.5 \sim 3.5)n_0$, but below we shall relax the condition and use only the range $n_B \simeq (1.5 \sim 2)n_0$, which corresponds to $\mu_{\rm q} = (340 \sim 345)$ MeV (i.e., $\mu_{\rm B} = (1.02 \sim 1.035)$ GeV). Then the 2SC pressure can be stiffer than before in the range of $n_B \simeq (2 \sim 3.5)n_0$. It is reasonable to stop fitting at $\mu_{\rm B} = 1.035$ GeV, because the baryon density is $n_B \simeq 2n_0$ beyond which APR is no longer reliable.

To satisfy the boundary conditions, i.e., the smooth connection to APR in the lower-density side and to the CFL phase with $G_{\rm v} \gtrsim 0.5G_{\rm s}$ in the higher-density side, we modify $G_{\rm v}(\mu_{\rm B})$ from an inverse logarithm to the following form:

$$G_{\rm v}(\mu_{\rm B})/G_{\rm s} = \frac{a}{\log[(\mu_{\rm B} - b)/c]} + d \qquad (4)$$

with an offset by d. Once we fix d, we can determine other three parameters, a, b, c using the smooth connection to APR. We changed d to find that the massive neutron star with $M > 2M_\odot$ is impossible with $d \lesssim 0.3$. We shall therefore choose $d = 0.4$ throughout this work. The parameters fixed in such a way, for $H = 1.5G_{\rm s}$ and $1.6G_{\rm s}$ respectively, are listed in Tab. 1 and the corresponding $G_{\rm v}(\mu_{\rm B})$ that interpolates between APR and the CFL phase is overlaid by dashed curves in Fig. 1.

With this running-$G_{\rm v}$ we can find the CFL solution as well as the 2SC phase and then we can locate a first-order phase transition between them by comparing the pressure. In Fig. 3 we show an example for $H = 1.5G_{\rm v}$ to find a first-order phase transition at $\mu_{\rm B} = 1.31$ GeV where the pressure of the interpolating 2SC phase with running $G_{\rm v}$ and the CFL phase crosses. We make a remark on the connection between APR and the 2SC phase around $\mu_{\rm B} \sim 1$ GeV. From Fig. 3 one might think that APR has a slightly larger pressure above the fitting region, and so APR would be rather favored. To resolve such confusion we here again emphasize our picture of the quarkyonic scenario. The change from NM to QM is not any phase transition but what we assume is a dual regime around $\mu_{\rm B} \sim 1$ GeV in which NM is gradually taken over by QM. In contrast to this smooth crossover from NM to QM, the change from the 2SC phase to the CFL phase is a genuine physical phase transition with different symmetry-breaking patterns. In many model studies including the present work, this phase transition turns out to be of first order.

$H/G_{\rm s}$	d	a	b [GeV]	c [GeV]
1.5	0.4	0.05283	0.4049	0.5735
1.6	0.4	0.1127	0.2942	0.6804

Table 1: Parameters for the interpolating $G_{\rm v}(\mu_{\rm B})$ between APR and the CFL phase.

Now that we have the EoS for the whole range of $\mu_{\rm B}$ from NM to CSC, we can compute not only the pressure P but the energy $\varepsilon = \mu_{\rm B} n_{\rm B} - P$ as well. Actually, the relation of P vs ε is essential for the estimation of the neutron star mass. Because ε involves a first derivative in $n_{\rm B}$, its value jumps discontinuously at the first-order phase transition. We can see this behavior in our numerical results shown in Fig. 4. It is also clear in Fig. 4 that the 2SC part hardly changes with different choices of H. We can explain this minor dependence from the fact that we impose the same boundary condition of APR at lower density. The other boundary condition of the CFL phase side is, on the other hand, loosely constrained by APR, and so there remains H dependence in the CFL part as is the case in Fig. 4. But as we will see below, the value of H is constrained by the causality condition.

One can deduce the sound velocity (squared) $c_s^2 = \partial P/\partial\varepsilon$ from the slope of curves in Fig. 4. We can numerically take the derivative of P with respect to ε and present obtained c_s^2 in Fig. 5. It is important to check the causal condition that c_s^2 should not exceed the unity (i.e., the speed of light in the natural unit). In the present setup, as understood from Fig. 5, the causality is not violated.

The structure of c_s^2 is almost the same irrespective of the choice of H; with increasing ε it monotonically increases in the APR region and then has a peak in the 2SC phase. Once a first-order phase transition to the CFL phase occurs, c_s^2 is pushed down to ~ 0.5. In the limit of large ε or high baryon density, c_s^2 asymptotically approaches ~ 0.6 which slightly depends on H. An interesting observation in Fig. 5 is that the peak height strongly depends on H and if H is greater than $\sim 1.6G_{\rm s}$, it would go beyond the unity, which would violate the causality. Therefore, such a large H is not allowed and $H = 1.6G_{\rm s}$ is close to the upper limit for our choice of $d = 0.4$ in Eq. (4). In this way we find that there is not much uncer-

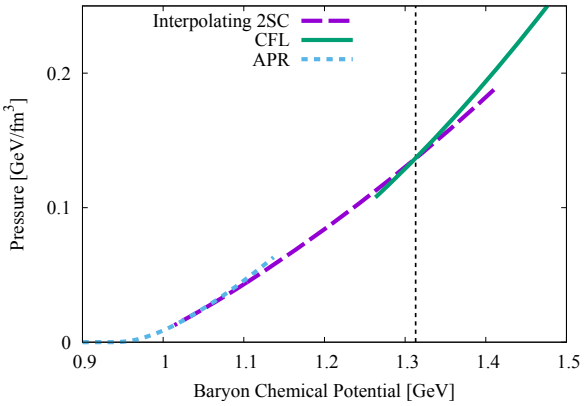

Fig. 3.— Pressure comparison of the 2SC phase (dashed curve) and the CFL phase (solid curve) for $H = 1.5G_{\rm s}$. The pressure of APR (dotted curve) is also shown for reference.

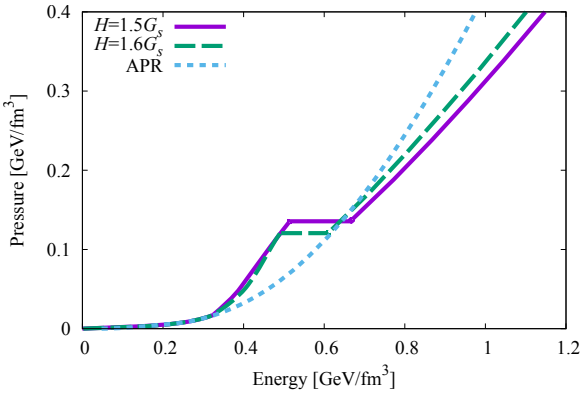

Fig. 4.— Pressure P as a function of the energy ε for $H = 1.5G_{\rm s}$ (solid curve) and $H = 1.6G_{\rm s}$ (dashed curve). The pressure of APR extrapolation (dotted curve) is shown for reference, though the plotted range is outside of its validity region.

tainty in the EoS determination after all.

Finally we comment on the connection of our result to the pQCD EoS. If we extrapolate our $P(\mu_B)$ curve to $\mu_B \sim 3$ GeV, it undershoots the pQCD pressure. This is not quite surprising: in the pQCD domain, one should expect smaller $G_{\rm s}$, $G_{\rm v}$, and H than those used in our analyses, since non-perturbative effects (gluons) are irrelevant by definition of the pQCD domain. By simply implementing the reduction of NJL parameters at large μ_B, one can connect our EoS to the pQCD EoS at $\mu_B \gtrsim 3$ GeV.

5. Mass-radius relation

To solve the M-R relation from the TOV equation what we need is the EoS shown in Fig. 4. Plugging our EoS to the TOV equation and changing the initial condition that is the central pressure at $r = 0$, we can get a curve in the plane of the mass and the radius of the neutron star as is just the standard procedure.

We summarize our results in Fig. 6. The M-R curves below $M_\odot$ are essentially determined by the APR EoS up to $n_{\rm B} \sim 2n_0$. (The tail at large R is determined by the crust EoS, for which we adopt the SLy model by Douchin & Haensel (2001).) Then, the 2SC curves start to take off from the APR by degrees. The 2SC curve's having the larger radii than the APR originates from a stiffer EoS in the 2SC phase at $n_{\rm B} > 2n_0$. In the vicinity of $M \sim 2M_\odot$ the curves have a turning point which signals the phase transition from the 2SC phase to the CFL phase. The maximal mass in our parametrization reaches $\simeq 2.2M_\odot$.

The neutron star radii at the canonical mass $1.4M_\odot$ typically spread over $R = (9 \sim 16)$ km, depending on the EoS for asymmetric nuclear matter. The radius of $R \simeq 12$ km in our results belongs to a group of small radii, reflecting that the APR at low density is softer than other typical hadronic EoS such as mean-field EoS. The small radii are consistent with recent observation that favors $R = (10 \sim 13)$ km (Ozel et al. 2010, 2015; Steiner et al. 2010, 2013), though those analyses still contain several assumptions to be verified. On the other hand there is also a group insisting $R > 14$ km (Suleimanov et al. 2011), which favors stiff hadronic EoS at low density (for hybrid EoS with stiff hadronic EoS, see e.g. Bonanno &

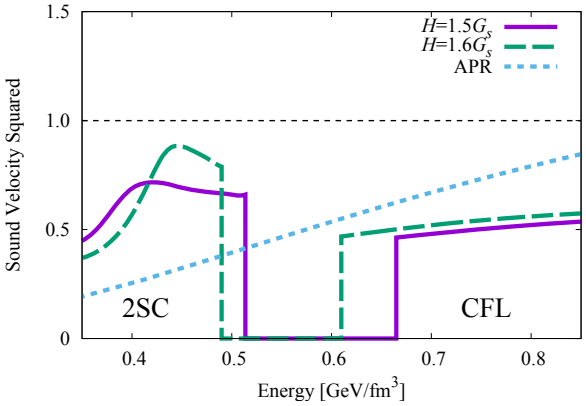

Fig. 5.— Sound velocity squared as a function of the energy for $H = 1.5G_{\rm s}$ (solid curve) and $H = 1.6G_{\rm s}$ (dashed curve). The APR extrapolation (dotted curve) is shown for reference.

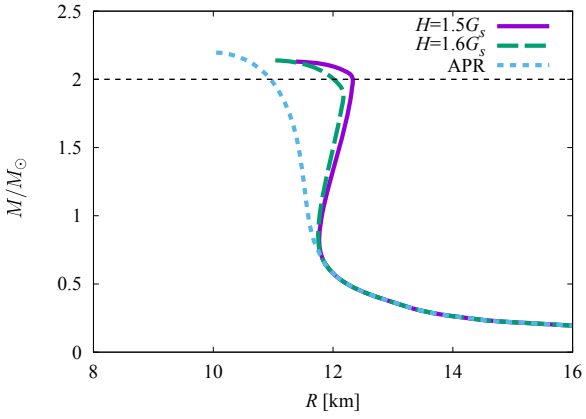

Fig. 6.— M-R relation for $H = 1.5G_{\rm s}$ (solid curve) and $H = 1.6G_{\rm s}$ (dashed curve). The APR result (dotted curve) is shown for reference.

Sedrakian (2012); Benic et al. (2015)). Another hint for the small radii comes from recent quantum Monte-Carlo calculations which indicate that nuclear EoS at low density is relatively soft, or even slightly softer than the APR (Gandolfi et al. 2012). The heavy-ion data by Danielewicz et al. (2002) also favor a soft EoS at low density.

Our crossover EoS yields relatively simple topology for the M-R curves similar to those in purely hadronic EoS. In case of the hybrid EoS with a first order phase transition, there are more varieties of the M-R curves. The classification was done by Alford et al. (2013); Alford & Han (2015), assuming the constant speed of sound.

6. Conclusions

Quarkyonic matter is a likely candidate to bridge a gap between nuclear matter and quark matter. It is an intermediate state of matter with a duality region that is describable by baryons or quarks. Thus, the EoS construction is not a patchwork of distinct EoS's of nuclear and quark matter, as is a conventional hybrid description having first-order phase transitions.

We discussed the interplay among quarks, diquarks, and baryons. Through processes of exchanging mesons or quarks between baryons, the diquark correlation develops in the intermediate state. While the density is low, the diquark is combined with other colored excitations to form local and color-singlet objects. For this reason diquarks should become manifest increasingly as baryons involve more and more quark exchange. We classified scenarios of deconfinement crossover according to the diquark characters and addressed what quarkyonic matter implies.

To interpret the crossover EoS in the language of microscopic degrees of freedom, we introduced a running vector coupling for quark models, with which the quark-hadron duality is implemented in a practically feasible manner. The running coupling is constrained by the conventional nuclear EoS in the low-density side and by massive neutron stars with $M > 2M_\odot$ in the high-density side. Because the idea is quite generic, one can employ any quark models and we adopted an NJL-type model for a concrete demonstration in this work.

The important finding is that the model parameters around $n_{\rm B} \sim 10n_0$ must be comparable with

those in the vacuum (i.e. matter at $\sim 10n_0$ still belongs to a non-perturbative regime); otherwise, the $2M_\odot$ constraint is not satisfied. The upper bound of the diquark interaction comes from the causality condition. After all, there is not much uncertainty remaining in the parameter determination. In principle, all the interactions in the quark model are mediated by gluons, and so substantially large couplings require non-perturbative gluon dynamics. We need to clarify the origin of non-perturbative dynamics in the high-density limit in a similar sense to the high-temperature limit at which the magnetic sector is still confining.

In this paper we interpret the enhancement of many-quark (meson) exchanges at $n_B \gtrsim 2n_0$ as an indicator for a new state of matter. While we consider diquarks in this paper, another branch of our picture would be the condensation of mesonic objects since many mesons are available among baryons. Although the previous studies in hadronic models typically predicted strong first order phase transitions associated with meson condensed phases, recent studies in quark models indicate that the appearance of inhomogeneous mesonic condensates does not necessarily accompany strong first order phase transitions, thus can avoid the significant softening (Buballa & Carignano 2015). The Skyrme crystal descriptions at *high* density (Paeng et al. 2015) have some overlap with such quark descriptions since both of them can address several effects beyond purely hadronic descriptions, such as the structural change of hadrons.

In this work we focused on the bulk properties of matter, i.e., the EoS only. To explore the refined characters of matter and to promote the advantage of our proposed method, we should study transport processes such as the cooling problem involving the strangeness. We shall leave this for future works.

We thank G. Baym, K. Masuda, L. McLerran, and J. Wambach for insightful conversations during Quark Matter 2015 in Kobe. This work was partially supported by JSPS KAKENHI Grants No. 15H03652 and 15K13479 (K. F.) and by NSF Grants PHY09- 69790 and PHY13-05891 (T. K.).

REFERENCES

Abbott, B. P., et al. 2009, Rept. Prog. Phys., 72, 076901

Abuki, H., Hatsuda, T., & Itakura, K. 2002, Phys. Rev., D65, 074014

Akmal, A., Pandharipande, V. R., & Ravenhall, D. G. 1998, Phys. Rev., C58, 1804

Alford, M., Braby, M., Paris, M. W., & Reddy, S. 2005, Astrophys. J., 629, 969

Alford, M. G., Berges, J., & Rajagopal, K. 1999a, Nucl. Phys., B558, 219

Alford, M. G., & Han, S. 2015, arXiv:1508.01261

Alford, M. G., Han, S., & Prakash, M. 2013, Phys. Rev., D88, 083013

Alford, M. G., Rajagopal, K., & Wilczek, F. 1999b, Nucl. Phys., B537, 443

Alvarez-Castillo, D. E., Beni, S., Blaschke, D., & astowiecki, R. 2014, Acta Phys. Polon. Supp., 7, 203

Antoniadis, J., et al. 2013, Science, 340, 6131

Baym, G., & Chin, S. A. 1976, Phys. Lett., B62, 241

Beane, S. R., Chang, E., Cohen, S. D., et al. 2013, Phys. Rev., D87, 034506

Benic, S., Blaschke, D., Alvarez-Castillo, D. E., Fischer, T., & Typel, S. 2015, Astron. Astrophys., 577, A40

Blaschke, D., Grigorian, H., & Voskresensky, D. N. 2004, Astron. Astrophys., 424, 979

Blaschke, D., Klahn, T., & Voskresensky, D. N. 2000, Astrophys. J., 533, 406

Bonanno, L., & Sedrakian, A. 2012, Astron. Astrophys., 539, A16

Bratovic, N. M., Hatsuda, T., & Weise, W. 2013, Phys. Lett., B719, 131

Brauner, T., Fukushima, K., & Hidaka, Y. 2009, Phys. Rev., D80, 074035, [Erratum: Phys. Rev.D81,119904(2010)]

Bringoltz, B. 2009, Phys. Rev., D79, 125006

Buballa, M. 2005, Phys. Rept., 407, 205

Buballa, M., & Carignano, S. 2015

Buballa, M., et al. 2014, J. Phys., G41, 123001

Cardall, C. Y., Prakash, M., & Lattimer, J. M. 2001, Astrophys. J., 554, 322

Danielewicz, P., Lacey, R., & Lynch, W. G. 2002, Science, 298, 1592

Demorest, P., Pennucci, T., Ransom, S., Roberts, M., & Hessels, J. 2010, Nature, 467, 1081

Dexheimer, V. A., & Schramm, S. 2010, Phys. Rev., C81, 045201

Ding, H.-T., Karsch, F., & Mukherjee, S. 2015, arXiv:1504.05274

Douchin, F., & Haensel, P. 2001, Astron. Astrophys., 380, 151

Drews, M., & Weise, W. 2015, Phys. Rev., C91, 035802

Duncan, R. C., & Thompson, C. 1992, Astrophys. J., 392, L9

Epelbaum, E., Hammer, H.-W., & Meissner, U.-G. 2009, Rev. Mod. Phys., 81, 1773

Fiorilla, S., Kaiser, N., & Weise, W. 2012, Nucl. Phys., A880, 65

Fradkin, E. H., & Shenker, S. H. 1979, Phys. Rev., D19, 3682

Fraga, E. S., Kurkela, A., & Vuorinen, A. 2015

Freedman, B., & McLerran, L. D. 1978, Phys. Rev., D17, 1109

Freedman, B. A., & McLerran, L. D. 1977, Phys. Rev., D16, 1169

Fukushima, K. 2003, Annals Phys., 304, 72

—. 2004, Phys. Rev., D70, 094014

—. 2005, Phys. Rev., D72, 074002

—. 2008, Phys. Rev., D78, 114019

—. 2014, Nucl. Phys., A931, 257

Fukushima, K., & Hatsuda, T. 2011, Rept. Prog. Phys., 74, 014001

Fukushima, K., Khan, N., Pawlowski, J. M., & Strodthoff, N. 2015, work in completion

Fukushima, K., Kouvaris, C., & Rajagopal, K. 2005, Phys. Rev., D71, 034002

Fukushima, K., & Sasaki, C. 2013, Prog. Part. Nucl.Phys., 72, 99

Gandolfi, S., Carlson, J., & Reddy, S. 2012, Phys. Rev., C85, 032801

Glendenning, N. K., & Schaffner-Bielich, J. 1998, Phys. Rev. Lett., 81, 4564

—. 1999, Phys. Rev., C60, 025803

Gubankova, E., Schmitt, A., & Wilczek, F. 2006, Phys. Rev., B74, 064505

Hands, S., Kim, S., & Skullerud, J.-I. 2010, Phys. Rev., D81, 091502

Hatsuda, T., & Kunihiro, T. 1994, Phys. Rept., 247, 221

Hatsuda, T., Tachibana, M., Yamamoto, N., & Baym, G. 2006, Phys. Rev. Lett., 97, 122001

Hebeler, K., Lattimer, J. M., Pethick, C. J., & Schwenk, A. 2010, Phys. Rev. Lett., 105, 161102

Hell, T., & Weise, W. 2014, Phys. Rev., C90, 045801

Hietanen, A., Kajantie, K., Laine, M., Rummukainen, K., & Schroder, Y. 2009, Phys. Rev., D79, 045018

Holt, J. W., Rho, M., & Weise, W. 2014, arXiv:1411.6681

Hotokezaka, K., Kiuchi, K., Kyutoku, K., et al. 2013, Phys. Rev., D87, 024001

Hotokezaka, K., Kyutoku, K., Okawa, H., Shibata, M., & Kiuchi, K. 2011, Phys. Rev., D83, 124008

Huang, M., & Shovkovy, I. A. 2004a, Phys. Rev., D70, 051501

—. 2004b, Phys. Rev., D70, 094030

Inoue, T., Aoki, S., Doi, T., et al. 2012, Nucl. Phys., A881, 28

Karsch, F., & Satz, H. 1980, Phys. Rev., D21, 1168

Kitamoto, S., et al. 2014, arXiv:1412.1165

Kitazawa, M., Koide, T., Kunihiro, T., & Nemoto, Y. 2002, Prog. Theor. Phys., 108, 929

Kitazawa, M., Rischke, D. H., & Shovkovy, I. A. 2008, Phys. Lett., B663, 228

Klahn, T., Blaschke, D., Sandin, F., et al. 2007, Phys. Lett., B654, 170

Kojo, T. 2012, Nucl. Phys., A877, 70

—. 2015, arXiv:1508.04408

Kojo, T., & Baym, G. 2014, Phys. Rev., D89, 125008

Kojo, T., Powell, P. D., Song, Y., & Baym, G. 2015, Phys. Rev., D91, 045003

Krueger, T., Tews, I., Hebeler, K., & Schwenk, A. 2013, Phys. Rev., C88, 025802

Kurkela, A., Romatschke, P., & Vuorinen, A. 2010, Phys. Rev., D81, 105021

Lastowiecki, R., Blaschke, D., Fischer, T., & Klahn, T. 2015, arXiv:1503.04832

Lattimer, J. M., & Prakash, M. 2001, Astrophys. J., 550, 426

—. 2007, Phys. Rept., 442, 109

Lonardoni, D., Lovato, A., Gandolfi, S., & Pederiva, F. 2015, Phys. Rev. Lett., 114, 092301

Masuda, K., Hatsuda, T., & Takatsuka, T. 2013a, Astrophys. J., 764, 12

—. 2013b, PTEP, 2013, 073D01

—. 2015, arXiv:1508.04861

McLerran, L., & Pisarski, R. D. 2007, Nucl. Phys., A796, 83

Nagae, T. 2010, Prog. Theor. Phys. Suppl., 185, 299

Nakazawa, K., & Takahashi, H. 2010, Prog. Theor. Phys. Suppl., 185, 335

Nishida, Y., & Abuki, H. 2005, Phys. Rev., D72, 096004

Nishizaki, S., Takatsuka, T., & Yamamoto, Y. 2002, Prog. Theor. Phys., 108, 703

Ohashi, Y., & Griffin, A. 2002, Phys. Rev. Lett., 89, 130402

Olausen, S. A., & Kaspi, V. M. 2014, Astrophys. J. Suppl., 212, 6

Ozel, F., Baym, G., & Guver, T. 2010, Phys. Rev., D82, 101301

Ozel, F., Psaltis, D., Guver, T., et al. 2015, arXiv:1505.05155

Paeng, W.-G., Kuo, T. T. S., Lee, H. K., & Rho, M. 2015, arXiv:1508.05210

Page, D., Geppert, U., & Weber, F. 2006, Nucl. Phys., A777, 497

Page, D., Lattimer, J. M., Prakash, M., & Steiner, A. W. 2004, Astrophys. J. Suppl., 155, 623

Page, D., Prakash, M., Lattimer, J. M., & Steiner, A. W. 2011, Phys. Rev. Lett., 106, 081101

Rajagopal, K., & Wilczek, F. 2000, arXiv:hep-ph/0011333

Rischke, D. H., Son, D. T., & Stephanov, M. A. 2001, Phys. Rev. Lett., 87, 062001

Sasaki, C., Friman, B., & Redlich, K. 2007, Phys. Rev., D75, 074013

Schaefer, T., & Wilczek, F. 1999, Phys. Rev. Lett., 82, 3956

Schon, V., & Thies, M. 2000, Phys. Rev., D62, 096002

Shternin, P. S., Yakovlev, D. G., Heinke, C. O., Ho, W. C. G., & Patnaude, D. J. 2011, Mon. Not. Roy. Astron. Soc., 412, L108

Steiner, A. W., Lattimer, J. M., & Brown, E. F. 2010, Astrophys. J., 722, 33

—. 2013, Astrophys. J., 765, L5

Suleimanov, V., Poutanen, J., Revnivtsev, M., & Werner, K. 2011, Astrophys. J., 742, 122

Sun, G.-f., He, L., & Zhuang, P. 2007, Phys. Rev., D75, 096004

't Hooft, G. 1974, Nucl. Phys., B75, 461

Tamura, H. 2010, Prog. Theor. Phys. Suppl., 185, 315

Tsubakihara, K., Maekawa, H., Matsumiya, H., & Ohnishi, A. 2010, Phys. Rev., C81, 065206

Tsuruta, S., Teter, M. A., Takatsuka, T., Tatsumi, T., & Tamagaki, R. 2002, Astrophys. J., 571, L143

Vidana, I., Logoteta, D., Providencia, C., Polls, A., & Bombaci, I. 2011, Europhys. Lett., 94, 11002

Weinberg, S. 1990, Phys. Lett., B251, 288

Weissenborn, S., Chatterjee, D., & Schaffner-Bielich, J. 2012, Phys. Rev., C85, 065802, [Erratum: Phys. Rev.C90,no.1,019904(2014)]

Yamamoto, Y., Furumoto, T., Yasutake, N., & Rijken, T. A. 2014, Phys. Rev., C90, 045805

This 2-column preprint was prepared with the AAS LaTeX macros v5.2.